ROYAL SOCIETY OF CHEMISTRY

PAPER

Upcycling of lithium cobalt oxide to $LiNi_{1/3}Mn_{1/3}Co_{1/3}O_2$†

Tristan Kipfer,[a] Jorge D. Gamarra,[a] Chunyan Ma, [b] Amanda Rensmo, [a] Laura Altenschmidt,[a] Michael Svärd, [b] Kerstin Forsberg [b] and Reza Younesi [*a]

With the increasing demand for rechargeable lithium-ion batteries arises an interest in the recycling processes for such devices. Possible methods include a range of processing conditions yielding different precursors which need to be integrated into upstream production. Here, we demonstrate a synthesis method that is compatible with the organic precursor obtained from citric acid-based leaching of lithium cobalt oxide (LCO) followed by acetone antisolvent crystallization. A lithium cobalt citrate (LCC) precipitate is retrieved and used directly as a precursor to synthesize $LiNi_{1/3}Mn_{1/3}Co_{1/3}O_2$ (NMC111) *via* a sol–gel method. The organic precursor is the only source of Co and provides a portion of the Li, while complementary metal salts supply the remaining metals in stoichiometric amounts. The role of metal salts (either acetates or sulfates of Ni, Mn and Li) is evaluated based on chemical composition and material purity. Electrochemical evaluation of the material produced from metal acetates shows comparable performance to that from a control material. The work connects previously studied methods of downstream leaching and antisolvent extraction with the upstream production of a desired cathode material through sol–gel synthesis. It is shown that our concept provides a path for avoiding primary and hazardous extraction of cobalt as the citrates obtained from acetone antisolvent crystallization of LCO can be applied as precursors for NMC111 synthesis, with few steps and applying only non-toxic solvents.

Sustainability spotlight

The transition from a linear to a circular economy is highlighted in the UN's SDG 7: Affordable and Clean Energy, among others. In this context, recycling processes for lithium-ion batteries are encompassed, not only because the scarcity of the required metals may result in a higher price for the clean energy enabled by the battery, but also because mining of specifically cobalt is at risk of violating human rights as well as increasing the environmental impact. Our method applies an upcycling aspect, where the metals from the now less used lithium cobalt oxide ($LiCoO_2$) cathode material are reintroduced into a more commercially viable cathode material based on lithium nickel manganese cobalt known as NMC. In addition, the process does not involve chemicals with implications for safety and environment or release of harmful emissions.

1 Introduction

Lithium-ion batteries (LIBs) are the backbone of the electrification of transport networks and are projected to be present in even larger amounts in several technologies. LIB-based energy storage capacity has grown from about 27 GW h (2009) to about 218 GW h (2019) with a current capacity around 600 GW h (2023).[1] It is expected that this growth rate will be sustained over the next decade, with more than 2500 GW h projected to appear on the market by 2030, depending on choice of scenario.[1,2] This market growth has just begun to result in a significant mass of critical raw material entering into the battery end-of-life stages, as the life expectancy of LIBs in electric vehicles (EVs) is above 10 years and through the inclusion of those with shorter life-times such as portable batteries in consumer products as well as scrap material from LIB production facilities.[3–5] Thus, it has become even more essential to cultivate processes to contain the valuable elements from battery waste in the market loop *via* recycling.[4,6]

Lithium cobalt oxide (LCO) was the cathode material of the first generation of LIBs. Investigated for its intercalation ability of Li, K. Mizushima and J. B. Goodenough published their result of a "new cathode material"[7] in 1980 and the first commercial rechargeable Li-ion battery was released on the market in 1991.[8] Since then, LCO has fallen out of favor on the market, especially for EVs, as cathodes containing nickel and manganese offer higher capacities and lower costs than cobalt dominated cathodes.[5,9–11] In addition, mining of the toxic cobalt is connected to human rights violations and child labor, most

[a]*Department of Chemistry-Ångström Laboratory, Uppsala University, Box 538, 75121, Uppsala, Sweden. E-mail: reza.younesi@kemi.uu.se*

[b]*Department of Chemical Engineering, KTH Royal Institute of Technology, Teknikringen 42, 11428 Stockholm, Sweden*

prevalent in the unstable Democratic Republic of the Congo accounting for the majority of the world's total resources.[3,11-16] Still, cobalt is present in the market-dominating cathode material in the form of lithium nickel manganese cobalt oxide (NMC) although in lower amounts.[2,9] With the increasing need for LIBs and thus for cobalt, upcycling of LCO into NMC would be a desired approach in a circular economy to utilize the cobalt present in the current waste streams of LCO.

As the first generation of large scale LIBs enter the waste stream, pyrometallurgical and hydrometallurgical recycling processes specific to lithium-ion batteries are promoted.[4,17] Current approaches include the shredding of the active components of the battery to produce what is commonly known as "black mass" from which the valuable metals (Ni, Mn, Co and Li) are extracted using different methods, mainly through heat or acid treatments.[3,4] The industrial processes were initially mainly based on pyrometallurgy. However, in recent years, larger focus has been placed on developing the hydrometallurgical methods to increase the recycling yield of lithium and decrease energy use, among other aspects.[4,18,19] In most of these hydrometallurgical processes, the black mass is subjected to strong inorganic acids that dissolve the metals which then are recovered *via* different purification and recovery techniques.[4,17,19,20] NH_3 or NaOH could also be applied in the process to control the pH or as precipitation agents.[17,19,21] In sum, leaching takes place in hydrometallurgy.

However, some of the added chemicals can cause release of poisonous gas or industrial safety issues among other aspects.[22,23] These complex processes may be examined with the aim to ease the application of the produced metal salts in the synthesis of new cathode materials, *e.g.*, with organic acids which degrade without toxic emissions.[22] A recent study by Cerrillo-Gonzalez *et al.*[22] demonstrate leaching of LCO with citric acid using copper as a reduction agent. Thus, in the absence of H_2O_2, the copper present in black mass could improve the acid dissolution and recovery yield. In addition, Xiao *et al.*[24] has shown the effective use of citric acid to leach both transition metals and lithium from NMC111 black mass with minimal pre-processing. There are also recent reports of solvent extraction and stripping of Ni, Co and Mn in citric acid media while applying ultrasound for process intensification.[25] Additionally, organic precursors for resynthesis of cathode materials can be recovered as precipitates *via* antisolvent crystallization as discussed by Xuan *et al.*[26] The use of citric acid in combination with antisolvent crystallization is therefore of interest as this could combine the advantages of limited toxicological hazards with simple processing and remanufacturing.

The successful integration of these downstream processes into the synthesis of materials would significantly simplify the flowsheet for cathode recycling while improving the upstream production. As several studies discuss various processes,[18,27-29] we here highlight two relevant synthesis methods. Co-precipitation is a common practice of NMC cathode material synthesis using materials recovered from spent LIBs, in which transition metal precursors (often either in the form of hydroxides or carbonates) are mixed in desired proportions. A chelating or precipitation agent such as NH_3 or NaOH is added while monitoring the pH.[18,27,28,30,31] However, for primary production of NMC cathodes or in the form of supplements, transition metal sulfate salts could be applicable.[32-36] Sintering is then applied after a lithium source is added (often in the form of carbonates obtained directly from LIB recycling or in the form of hydroxides originating from primary resources as well as converted precipitates from LIB recycling) followed by calcination.[18,28] Advantages with co-precipitation are cost-effectiveness and scalability as well as the production of well-defined round agglomerates where the shape, morphology and particle shape are tunable by several parameters.[27,28]

In contrast, the sol–gel procedure consists of dissolving a stochiometric amount of the desired transition metals (for example in the form of acetates or nitrates) in distilled water and adding a chelating agent such as citric acid.[29,36-41] By stirring at an intermediate temperature with a fixed pH, the solution forms a gel which is then treated thermally and mechanically in several steps.[27,29] As a result, the material is produced at lowered process temperatures and of homogeneous composition with controlled morphology and uniform particle size distribution. The method could therefore be of interest with materials requiring high surface area.[27,29] As an example, Çetin *et al.*[37] utilized citric acid as a chelating agent and transition metal acetates when preparing an NMC material by the sol–gel method. While co-precipitation is a better solution than the sol–gel method for upscaling in general,[18,27-29] the citrate concentration for the former has an optimal ratio of max 0.01 (citrate to metal ions)[23] whereas the latter can tolerate up to 2 equivalents.[37] In fact, when using organic acids as leaching agents, the sol–gel method is more applicable as the organic acid also acts as a chelating agent.[20]

Here, the synthesis of the NMC111 cathode material *via* the use of organic precursors obtained from recovered precipitates of upcycled LCO is investigated. In short, during sol–gel synthesis either metal acetates or metal sulfates (Ni, Mn and additional Li) were added to mixed metal precipitates (Co and Li) obtained from citric acid leaching of LCO followed by antisolvent crystallization of metal citrates. The innovation in this research lies in utilizing citrates directly, without necessitating their conversion into carbonates or hydroxides. The work highlights the benefits of a sol–gel synthesis using complementary nickel, manganese, and lithium acetate salts with the citric acid-based precursors. Secondly, it provides a proof-of-concept method to utilize the cobalt in a refined process for separate handling of discarded LCO batteries. As a result, it is possible to develop LCO upcycling processes that require only non-toxic chemicals before being implemented in the production of NMC111, utilizing no primary resource of cobalt.

2 Materials and methods

The proposed method consists of a number of steps where pure LCO underwent downstream and upstream production of NMC111, see Fig. 1. For the recovery of Li and Co, $LiCoO_2$ was leached by a solution of citric acid and then precipitated using acetone antisolvent crystallization (downstream). The obtained precursor was resynthesized into NMC, using the lithium cobalt
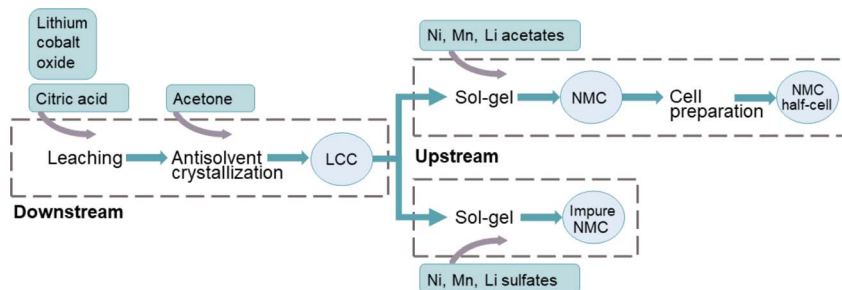
Fig. 1 Graphical scheme of the downstream and upstream processes of upcycling LCO to NMC111, comparing utilization between complementary metal salts in sol−gel processing, denoted as the acetate route (top) or sulfate route (bottom). LCC refers to lithium cobalt citrate. The (im)purity of the produced NMC is further discussed below, see *e.g.*, the discussion of the normalized XRD diffraction patterns.

citrate (LCC) precipitate together with complementary metal acetate or sulfate salts in a sol–gel process (upstream).

2.1 Materials

Downstream processes included citric acid ($C_6H_8O_7$, ≥99.5%) and acetone (C_3H_6O ≥99%) as well as the material to be recovered, lithium cobalt oxide ($LiCoO_2$, ≥99.8%). Lithium acetate dihydrate ($C_2H_3O_2Li\cdot2H_2O$, ≥99.0%), nickel acetate tetrahydrate ($C_4H_6NiO_4\cdot4H_2O$, ≥98%) and manganese acetate tetrahydrate ($C_4H_6MnO_4\cdot4H_2O$, ≥99%) or lithium sulfate monohydrate ($Li_2SO_4\cdot H_2O$, ≥99.0%), nickel sulfate hexahydrate ($NiSO_4\cdot6H_2O$, ≥98.5%) and manganese sulfate monohydrate ($MnSO_4\cdot H_2O$, ≥99%) were used in the upstream production of new batteries. For production of half-cells, 1.0 M $LiPF_6$ in ethylene carbonate and dimethyl carbonate (EC/DMC in 50/50 (v/v) ratio) and *N*-methyl-2-pyrrolidone (NMP) were used. All the chemicals were purchased from Sigma Aldrich except technical acetone retrieved from VWR, and used without further purification. The mono-element standards of Li, Co, Ni, and Mn (1000 mg L^{-1} in 2–5% HNO_3) were purchased from VWR chemicals for inductively coupled plasma-optical emission spectrometry (ICP-OES) analysis of leaching samples.

2.2 Downstream

Lithium cobalt oxide was leached using a 1.5 M citric acid aqueous solution in a solid to liquid ratio of 25 g L^{-1} by soni-cation at 60 °C for 48 hours. The citrate-based precursor was recovered from the leach liquor by slow addition of an equal volume of acetone to the leachate using antisolvent crystallization with acetone as described by Xuan *et al.*[26] The resulting solution was left to crystallize for 48 hours at room temperature after which it was filtered. In addition, nine samples from the leach solution were collected at specified times for a period of 70 hours, for a total of three experimental runs. Each sample was collected with a syringe and filtered using syringes equipped with membrane filters (VWR, pore size of 0.2 mm, PTFE) upon sampling.

2.3 Upstream

The sol–gel procedure used in this work is an adaptation of the methodology described by Çetin *et al.*[37] After determining the composition of the organic LCC precursor from antisolvent crystallization, a stoichiometric ratio of Ni, Mn and Co (1 : 1 : 1) was dissolved in distilled water, where the Co from the LCC precipitate was mixed with either Ni and Mn acetate salts (acetate route) or Ni and Mn sulfate salts (sulfate route). Li was added in the form of lithium acetate or lithium sulfate, respectively, to reach a molar ratio of Li to total transition metal of 1.05 together with an adequate amount of citric acid to reach two molar equivalents to the organic precursor. The solution was stirred at 250 rpm and heated at 65 °C until the water evaporated. The resulting powder was ground and calcined, first at 350 °C for four hours in a quartz tube furnace and then again before a second calcination step at 900 °C for another ten hours, all under oxygen flow (0.5 L min^{-1}).

2.4 Characterization methods

2.4.1 ICP-OES. The metal content of the downstream precipitate was determined *via* induction coupled plasma-optical emission spectroscopy (ICP-OES) using a Thermo Scientific iCAP 7000plus. The solid sample was first dissolved in an aqueous HNO_3 solution of 5% v/v of the concentrated (69.5% w/w) HNO_3 (69.5% w/w) in a solid to liquid ratio of 1 mg mL^{-1} until a clear solution was formed. After that, the resulting liquid sample was further diluted with Milli-Q water to obtain metal concentrations within the detection limit of the instrument. The mass-based dilution was employed to minimize errors introduced during the dilution process. The liquid samples collected during leaching were diluted with aqueous HNO_3 at a mass-based dilution factor of approximately 100 to maintain the metal concentrations within the quantification range of ICP-OES. The mass of each sample before and after dilution was precisely recorded to obtain the accurate mass-based dilution factor. Mass-based standards used in the ICP measurement were prepared by diluting concentrated metal standards at specific mass-based dilution factors. Following that, the mass-based metal concentration, representing the metal content per unit mass of the leaching solution, was obtained and used in this work. Similarly, the upstream NMC powder was analyzed through ICP-OES.

2.4.2 Raman spectroscopy. The downstream precipitate was analyzed using a Micro-Raman spectroscopy system (Renishaw Invia, Wotton-under-Edge, UK) equipped with

a 785 nm excitation laser. A deep-depletion charge-coupled device detector was used for signal collection and spectra were measured with a 20× objective (numerical aperture = 0.4; Leica, Wetzlar, Germany). The laser power density at the sample plane was ~0.1 mW m^2 using standard mode. The extended scan spectra with a spectral range of 400–1800 cm^{-1} were obtained using the exposure time of 20 seconds and two times of accumulation. The software package WIRE 2.0 (Renishaw Invia) was used for spectral acquisition and the rapid removal of spurious peaks. Control of the system performance was achieved using a silicon wafer peak at 520 cm^{-1} before and during the experiment.

2.4.3 XRD. The crystal structure of the downstream and upstream samples was analyzed using a Bragg–Brentano geometry Siemens D5000 X-ray diffractometer with a Cu K$_\alpha$ (1.5406 Å) and K$_\beta$ (1.5443 Å) radiation at 40 kV and 40 mA. The sample preparation consisted of a wet grinding in ethanol. The ethanol dispersion was then deposited on a clean silicon surface and dried at room temperature. A scan speed of 0.6° min^{-1} within a range of 10 to 90° and an increment of 0.02° was applied.

2.4.4 Scanning electron microscopy. The morphology of the upstream samples was analyzed using a microscope Zeiss 1550 with an InLens detector. The sample was deposited on a conductive carbon plate and then placed in the chamber. The electron beam energy was varied from 5 to 20 kV.

2.4.5 Half-cell cycling. NMC111 powder from the acetate route, as described in Fig. 1, was mixed with 5% of PVdF in NMP solution and carbon black in an 8:1:1 ratio, and then ball-milled for 30 min at 30 Hz. An aluminum sheet with a thickness of 250 μm was covered with the obtained slurry and dried overnight at 70 °C in a vacuum oven. Afterwards, electrodes were punched to 13 mm diameter and dried again at 120 °C inside a glove box for 12 hours using a Büchi oven. The NMC111 mass loading ranged between 5 and 6 mg cm^{-2}. Pouch cells were assembled using a metallic Li sheet as the anode, and 100 μL of the LiPF$_6$ in EC/DMC 50/50 electrolyte. For the separators, 2 sheets of Celgard 2500 were used. For comparison, a "control" cell was tested using the same electrode and cell preparation procedures using an NMC111 material from CustomCells. Assembled cells were allowed to rest for 10 hours and were then cycled 50 times between 2.8 V and 4.2 V using a C-rate of C/2.5 using an ARBIN cycling equipment. At least three half-cells were measured for each sample from the acetate route as well as for the control material.

3 Results and discussion

3.1 Downstream

The downstream process as depicted in Fig. 1 is comprised of two sequential steps. The first involves leaching of LCO using citric acid. The leaching curve of metal concentration as a function of time for ultrasonic leaching of LCO using citric acid is shown in Fig. 2. Each resulting metal concentration value is an average of three repeated ICP-OES measurements. The results show that the cobalt concentration increases over time reaching a plateau with the concentration of 4978.84 ± 91.19 mg kg^{-1} after 50 hours of extraction, *i.e.*, 38.4 ± 0.7% of Co extracted into the solution. The lithium concentration increased over the studied time from 1019.62 ± 72.50 mg kg^{-1} (leaching efficiency of 66.8 ± 4.8%) after 50 hours to 1286.56 ± 53.84 mg kg^{-1} (leaching efficiency of 84.3 ± 3.5%) after 72 hours with no sign of a plateau. The concentration of the leach liquor is similar to that of lithium and cobalt as those from NMC111 as shown by Xuan *et al.*[26] and those of pure LCO as presented by Cerrillo-Gonzalez *et al.*[22]

The leaching with monoprotic organic acids is often performed in the presence of H$_2$O$_2$, acting as a reducing agent, to increase the leaching efficiency of the organic acid.[19] In the present study, no additional reducing agent was used. Here, we use ultrasonication responsible for the formation of cavitation and increased diffusion of the leaching agent, resulting in an increased leaching efficiency.[24,26] Furthermore, previous studies report on the possibility of citric acid acting not only as
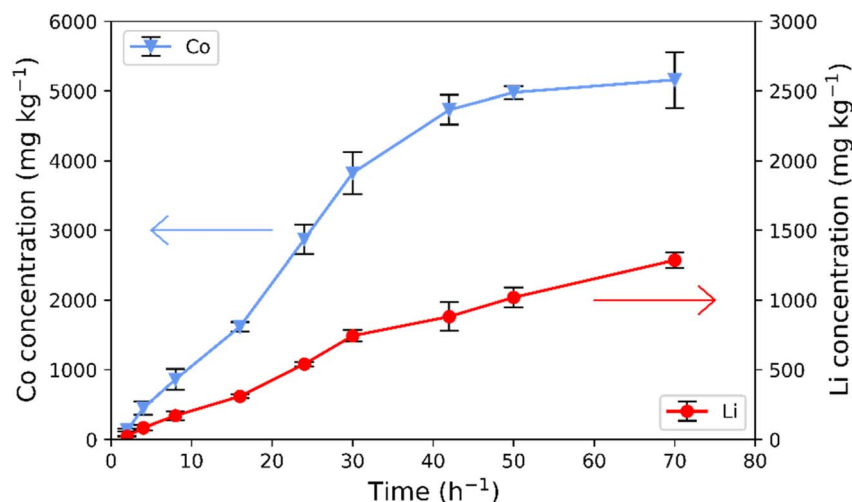

Fig. 2 Metal concentration as a function of time during leaching of Co (blue) presented on the primary *y*-axis and Li (red) presented on the secondary *y*-axis. Error bars represent the deviation of three leaching experiments.

a chelating agent but also as a mild reducing agent. In that case, the citric acid was oxidized into dicarboxyacetone *via* a decarboxylation.[43,44] The possible reduction mechanism in the case of LCO with citric acid remains to be determined.

After leaching, antisolvent crystallization using acetone as an antisolvent was applied, as illustrated in Fig. 1. The metal concentration (Li and Co) of the precipitates was analyzed by ICP-OES with each resulting metal concentration value as an average of three repeated ICP-OES measurements. By assuming the formation of metal anhydrous citrate, the amount of citrate in the solid was calculated by subtracting the metal mass from the total mass of the product. The final concentrations of lithium and cobalt in the solid sample are 0.964 ± 0.014 mmol g^{-1} and 3.5758 ± 0.0061 mmol g^{-1} of precipitate, respectively, whereas the citrate concentration is calculated to be 4.073 ± 0.058 mmol g^{-1}. This translates into a total metal to citrate ratio of roughly one. The specific complex formed cannot be elucidated *via* this approach, but it leaves the possibility of a mixture of lithium citrates and cobalt citrates or a lithium cobalt citrate (LCC) precipitate.

It is important to note that in the case of actual recycled LCO cathodes, the components such as Al and Cu, originating from current collectors, inevitably affect the leaching process, resulting in a solution containing Cu and Al.[22,26] Previous studies[45] have demonstrated that the presence of Cu and Al (6.4 mol% metal base) in the organic acid-based NMC precursor leads to a notable decrease in discharge capacity. Therefore, it is essential to remove impurities before leaching, reduce impurity levels by controlling the antisolvent crystallization process, or further purify the precipitates from the antisolvent step to decrease the impurity content. Still, as the presence of Cu is shown to increase the recycling yields of Li and Co,[22,42] leaching of black mass rather than pure lithium cobalt oxide could possibly increase the yields measured in this work. Herein, LCO was chosen in this stage to demonstrate the concept of upcycling. Clearly, further investigation into reducing impurity levels to acceptable thresholds in future work is necessary to apply it in battery recycling.

The recovered LCC precipitate is further characterized by Raman spectroscopy and compared to the spectra of citric acid, see Fig. 3. The spectrum of the LCC precipitate does not fully present the typical spectral features of citric acid; rather it is characterized by a set of broader and displaced bands compared to the defined peaks of citric acid. For the LCC precipitate, many of the distinctive bands of citric acid such as the carboxylate symmetric stretching band, $\nu_s(COO)$[46,47] around 1400 cm^{-1}, are broadened. This suggests the presence of interactions between the carboxylic groups of the citrate with the different metal ions and the formation of complexes. In addition, the $\nu(C=O)$[47] band between 1691 and 1735 cm^{-1} and the deformation modes, $\nu(COO)$,[46] which are seen between 500 and 800 cm^{-1} in the citric acid spectra, are not visible in the spectra of the LCC precipitate. Additionally, citric acid in a complex will yield a spectrum with fewer visible peaks, as seen by Kartal *et al.*[47] for the $[CoK_4(\mu_{10}\text{-}C_6H_5O_7)_2]_n$ complex. This suggests that the LCC precipitate likely consists of lithium citrates and cobalt citrates, but other additional lithium and cobalt containing carboxylate salts cannot be excluded. Since a significant part of the peaks are broadened and weakened a more detailed description of the precipitate is inhibited. Nevertheless, the precipitates are water soluble, and are thus compatible with the synthesis approach used further on during the upcycling.

3.2 Upstream

The desired composition of the synthesized material in this work was NMC111. Although Ni-rich cathode materials are more common on the market today, as described above, this work provide a proof-of-concept of a method producing equal amounts of Co to other transition metals. This highlights the possibility of upcycling from LCO utilizing the resources efficiently, possibly in a single waste stream, which could be a stepping stone for further work. Thus, the LCC precipitate from antisolvent crystallization was further used in the upstream production as an organic precursor in the sol–gel synthesis method, either in the acetate route or sulfate route, as presented in Fig. 1. Samples produced using the two different complementary salts are compared by XRD. The normalized diffraction patterns from the two upstream methods can be seen in Fig. 4, in comparison to the one of the control sample and the diffraction lines of NMC111 (ICDD: 04-014-7636), Li_2SO_4 (ICDD: 00-020-0640) and $MnCoNiO_4$ (04-019-8823).

The reflections from the sample prepared by the acetate route (4a) are consistent with single phase NMC111 (4d, in dark red) as the expected reflections for a single-phase NMC111 (*e.g.*, (003) and (104)) are present without any other impurity peaks. In addition, the splitting of (006) and (012) reflections is clearly defined with a narrow profile of all diffraction lines for the acetate sample (replicate 2). Similarly, the control sample containing NMC111 (4c) is exhibiting a pattern with very close resemblance to that for the sample from the acetate route. On the other hand, the diffraction pattern for the sample from the sulfate route (4b) shows diffraction peaks inconsistent with the ones of NMC111. The peaks are consistent with the ones of lithium sulfate (4d, in yellow), one of the added precursors,
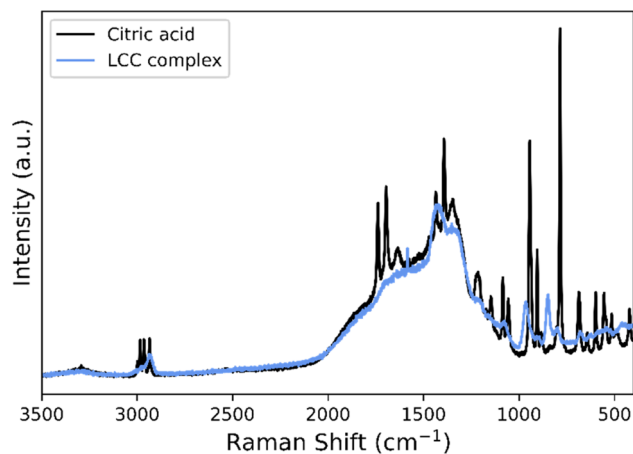
Fig. 3 Raman spectrum of the LCC precipitate (blue) in comparison to the spectrum of citric acid (black).
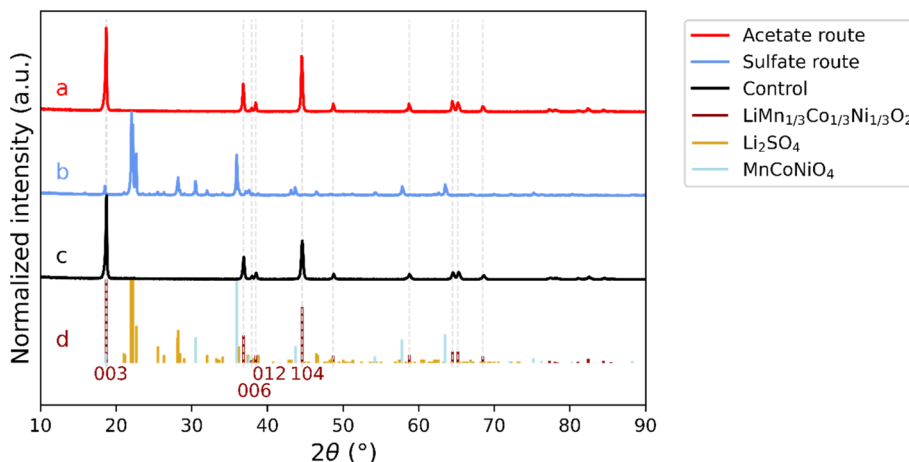
Fig. 4 Normalized XRD patterns from 10 to 90° 2Θ collected for samples from (a) the sulfate route and (b) the acetate route (below denoted as replicate 2), and (c) control NMC111. In (d) peaks for $LiMn_{1/3}Co_{1/3}Ni_{1/3}O_2$ (ICDD: 04-014-7636), Li_2SO_4 (ICDD: 00-020-0640) and $MnCoNiO_4$ (04-019-8823) are shown together with identification of relevant reflections (003, 006, 012 and 104) and dashed lines for comparison of the significant reflections in $LiMn_{1/3}Co_{1/3}Ni_{1/3}O_2$ (*i.e.*, NMC111) up to 70°.

which could be an effect of the strong chelating effect by sulfate on this material[48], as well as the mixed metal oxide phase $MnCoNiO_4$ (4d, in light blue). It can be noted that other phases consistent with various combinations of lithium oxides with either Ni, Co or Mn could be present. Within the scope of this work, no further identification was performed as the conclusion is clear that using metal sulfates for the LCC precipitate does not result in a single-phase NMC111. Thus, citric acid leaching and acetone antisolvent crystallization is not compatible with sol–gel using complementary metal sulfate salts.

The characterization by XRD does not only allow determination of the material's purity, but defects in the NMC crystal structure can also be estimated using peak ratios. For NMC111, this can be done using the ratio of the (003) to the (104) peaks, where a value larger than 1.2 indicates a well-ordered structure, with Li in its correct position without negative effects on the electrochemical performance.[49] Two replicates of samples from the acetate route (replicate 1 and replicate 2) were investigated with XRD and compared to each other as well as to the control sample, see Fig. S1.† The XRD patterns show that both replicate 1 and replicate 2 present a single-phase NMC111, where the peak ratio I_{003}/I_{104} is calculated to values of 1.49 (replicate 1) and 1.32 (replicate 2), which can be compared to a value of 1.58 for the control. The ratios are above 1.2 indicating a well-ordered structure. In addition, the well-defined splitting of the peaks (006) and (012), also seen in Fig. 4 for replicate 2,

suggests a minimal cation mixing and an ordered, layered structure.[31,49]

The metal content of the NMC111 prepared by the upstream process was further analyzed by ICP-OES. For the two replicates produced in the acetate route, the molar equivalence to Co is in average: 2.60 ± 0.48 (Li), 0.9765 ± 0.0042 (Ni) and 0.9966 ± 0.0086 (Mn). The molar equivalence between the transition metals is as expected for NMC111, although with a lower Li content than expected, possibly resulting from evaporation during the calcination process.

Apart from the crystal structure, the battery performance would also be influenced by the morphology of the particles of the active cathode material, which was studied by SEM for replicate 1 and replicate 2. Fig. 5 shows the difference in particle morphology between the control sample and the samples produced using metal acetates as determined with SEM at magnifications of 25k. The overall morphologies are comparable, with both materials exhibiting the expected two-stage morphology, that is, larger particles over a micrometer in size composed of an agglomerate of small oxide blocks. Control NMC111 shows agglomerates consistent with the morphology of the product of co-precipitation with a well-defined round shape,[27,28] while replicate 1 and replicate 2 have less definite particles likely resulting from the grinding process. The replicates together with the control have similar sized crystals around 200–300 nm offering similar active areas.
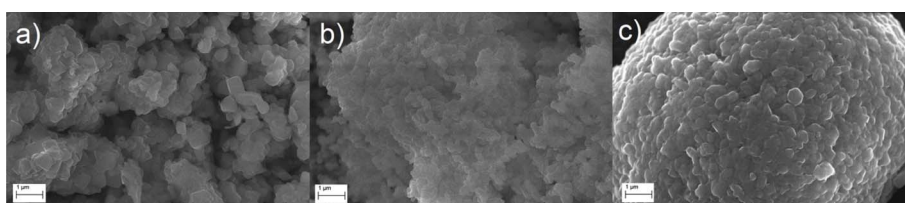

Fig. 5 SEM images of samples from the acetate route, namely (a) replicate 1 and (b) replicate 2 together with (c) the control at a magnification of 25k.
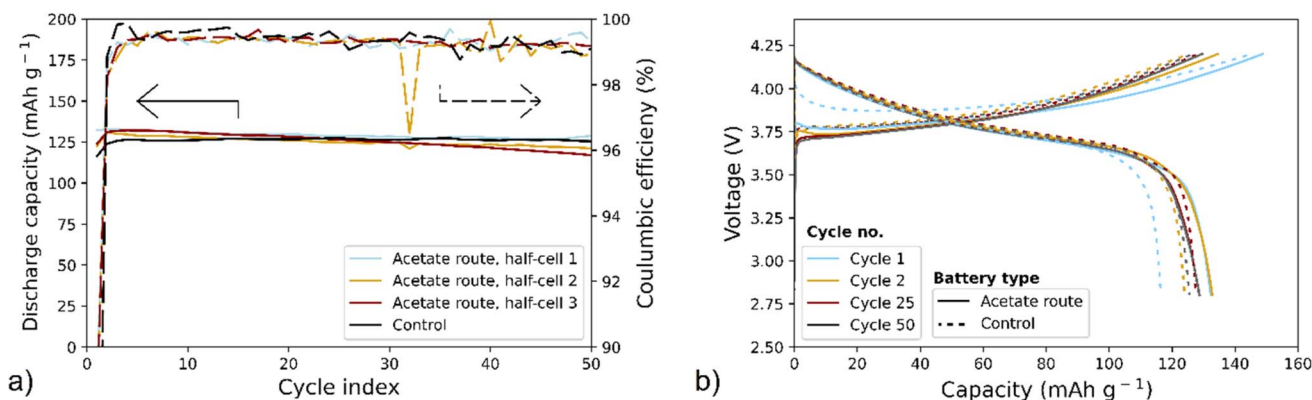
Fig. 6 Half-cell electrochemical cycling performance of NMC produced from the acetate route compared to the control NMC111 sample. (a) Discharge capacities and coulombic efficiencies of three half-cells using synthesized NMC compared to control NMC111, (b) charge–discharge profiles between 2.8 and 4.2 V for cycles 1, 2, 25, and 50 for the acetate route and the control.

For electrochemical evaluation, a set of half-cells using NMC produced *via* the acetate route (replicate 1 and replicate 2), see Fig. 1, were assembled and galvanostatically cycled for 50 cycles using C/2.5 rate. The control NMC111 was also electrochemically cycled with the same experimental parameters. For all the samples, cycling of at least 3 half-cells was repeated to ensure reproducibility of results. As shown in Fig. 6a, the average discharge capacities over 50 cycles are around 120–130 mA h g^{-1} while coulombic efficiencies are above 90%. Fig. 6b displays voltage profiles of cycling control NMC111 and NMC produced *via* the acetate route. The cells show similar discharge and charge voltage profiles as well as total discharge and charge capacities, however, the reversibility (*i.e.*, coulombic efficiency) of the 1st cycle of the synthesized NMC is higher than that of control NMC111 (see solid and dashed light blue lines in Fig. 6a). Overall, the electrochemical results indicate that the NMC produced *via* the acetate route provides similar performance to that of the control NMC111.

4 Conclusion

This work is a proof-of-concept of the upcycling of cobalt from LCO in a few steps using only abundant and safe chemicals providing a path of completely avoiding cobalt mining for battery production. The proposed scheme with the sol–gel approach has been shown to be compatible with precursors produced by the citric acid-based leaching using complementary metal acetate salts. With minimal preprocessing the material is upcycled into an NMC111 battery using 100% recycled Co. The morphology and crystal structure of the synthesized NMC are comparable to those of the control NMC111, with well-defined agglomerates and minimal cation mixing. Electrochemical measurements show that NMC111 produced *via* the acetate route provided a charge capacity of around 150 mA h g^{-1} at the 1st charge, followed by capacities of around 120–130 mA h g^{-1} in the following cycles, when cycled between 2.8 V and 4.2 V at C/2.5 rate. The electrochemical cycling results – in addition to the physical characterizations – confirm the similarity of the synthesized NMC111 to the control NMC111.

The stability of the material is not affected by the recycling process and citrates have been proven to be compatible in the sol–gel synthesis of the cathode material applying complementary metal acetate salts. NMC111 produced from this simplified upcycling process results in commercially viable materials, effectively keeping both lithium and cobalt from waste streams and in the production loop of new cathode chemistries.

To upgrade this proof-of-concept into an industrially applicable process, the proposed method should be further studied using black mass as feed. This work should also serve as an offset to continue with an investigation of sol–gel synthesis of LCO into other NMC chemistries with higher Ni content.

Conflicts of interest

There are no conflicts to declare.

Acknowledgements

References

1 H. E. Melin, M. A. Rajaeifar, A. Y. Ku, A. Kendall, G. Harper and O. Heidrich, Global implications of the EU battery regulation, *Science*, 2021, **373**, 384–387.

2 F. Degen, M. Winter, D. Bendig and J. Tübke, Energy consumption of current and future production of lithium-ion and post lithium-ion battery cells, *Nat. Energy*, 2023, **8**, 1284–1295.

3 G. Harper, R. Sommerville, E. Kendrick, L. Driscoll, P. Slater, R. Stolkin, A. Walton, P. Christensen, O. Heidrich,

S. Lambert, A. Abbott, K. Ryder, L. Gaines and P. Anderson, Recycling lithium-ion batteries from electric vehicles, *Nature*, 2019, **575**, 75–86.

4 J. Neumann, M. Petranikova, M. Meeus, J. D. Gamarra, R. Younesi, M. Winter and S. Nowak, Recycling of lithium-ion batteries—Current state of the art, circular economy, and next generation recycling, *Adv. Energy Mater.*, 2022, **12**, 2102917.

5 F. Maisel, C. Neef, F. Marscheider-Weidemann and N. F. Nissen, A forecast on future raw material demand and recycling potential of lithium-ion batteries in electric vehicles, *Resour., Conserv. Recycl.*, 2023, **192**, 106920.

6 J. Baars, T. Domenech, R. Bleischwitz, H. E. Melin and O. Heidrich, Circular economy strategies for electric vehicle batteries reduce reliance on raw materials, *Nat. Sustain.*, 2021, **4**, 71–79.

7 K. Mizushima, P. C. Jones, P. J. Wiseman and J. B. Goodenough, Li_xCoO_2 (0<x≤1): A new cathode material for batteries of high energy density, *Mater. Res. Bull.*, 1980, **15**, 783–789.

8 M. V. Reddy, A. Mauger, C. M. Julien, A. Paolella and K. Zaghib, Brief history of early lithium-battery development, *Materials*, 2020, **13**, 1884.

9 O. Winjobi, J. C. Kelly and Q. Dai, Life-cycle analysis, by global region, of automotive lithium-ion nickel manganese cobalt batteries of varying nickel content, *Sustainable Mater. Technol.*, 2022, **32**, e00415.

10 T. Ohzuku and Y. Makimura, Layered lithium insertion material of $LiNi_{1/2}Mn_{1/2}O_2$: A possible alternative to $LiCoO_2$ for advanced lithium-ion batteries, *Chem. Lett.*, 2001, **30**, 744–745.

11 S. S. Nisa, M. Rahmawati, C. S. Yudha, H. Nilasary, H. Nursukatmo, H. S. Oktaviano, S. U. Muzayanha and A. Purwanto, A fast approach to obtain layered transition-metal cathode material for rechargeable batteries, *Batteries*, 2022, **8**, 4.

12 C. Banza Lubaba Nkulu, L. Casas, V. Haufroid, T. De Putter, N. D. Saenen, T. Kayembe-Kitenge, P. Musa Obadia, D. Kyanika Wa Mukoma, J.-M. Lunda Ilunga, T. S. Nawrot, O. Luboya Numbi, E. Smolders and B. Nemery, Sustainability of artisanal mining of cobalt in DR Congo, *Nat. Sustain.*, 2018, **1**, 495–504.

13 P. Meshram, B. D. Pandey and Abhilash, Perspective of availability and sustainable recycling prospects of metals in rechargeable batteries – A resource overview, *Resour. Policy*, 2019, **60**, 9–22.

14 Amnesty International, *'This is what we die for' Human rights abuses in the Democratic Republic of the Congo power the global trade in cobalt*, Amnesty International, London, 2016.

15 Amnesty International, *Time to Recharge: Corporate Action and Inaction to Tackle Abuses in the Cobalt Supply Chain*, Amnesty International, London, 2017.

16 Amnesty International, *Powering Change or Business as Usual? Forced Evictions at Industrial Cobalt and Copper Mines in the Democratic Republic of the Congo*, Amnesty International, London, 2023.

17 E. Fan, L. Li, Z. Wang, J. Lin, Y. Huang, Y. Yao, R. Chen and F. Wu, Sustainable recycling technology for Li-ion batteries and beyond: Challenges and future prospects, *Chem. Rev.*, 2020, **120**, 7020–7063.

18 V. Verma, J. R. Joseph, R. Chaudhary and M. Srinivasan, Upcycling spent cathode materials from Li-ion batteries to precursors: Challenges and opportunities, *J. Environ. Chem. Eng.*, 2023, **11**, 110216.

19 T. Or, S. W. D. Gourley, K. Kaliyappan, A. Yu and Z. Chen, Recycling of mixed cathode lithium-ion batteries for electric vehicles: Current status and future outlook, *Carbon Energy*, 2020, **2**, 6–43.

20 L. Li, X. Zhang, M. Li, R. Chen, F. Wu, K. Amine and J. Lu, The recycling of spent lithium-ion batteries: A review of current processes and technologies, *Electrochem. Energy Rev.*, 2018, **1**, 461–482.

21 Y. Yao, M. Zhu, Z. Zhao, B. Tong, Y. Fan and Z. Hua, Hydrometallurgical processes for recycling spent lithium-ion batteries: A critical review, *ACS Sustain. Chem. Eng.*, 2018, **6**, 13611–13627.

22 M. del M. Cerrillo-Gonzalez, J. M. Paz-Garcia, M. Muñoz-Espinosa, J. M. Rodriguez-Maroto and M. Villen-Guzman, Extraction and selective precipitation of metal ions from $LiCoO_2$ cathodes using citric acid, *J. Power Sources*, 2024, **592**, 233870.

23 K.-M. Nam, H.-J. Kim, D.-H. Kang, Y.-S. Kim and S.-W. Song, Ammonia-free coprecipitation synthesis of a Ni–Co–Mn hydroxide precursor for high-performance battery cathode materials, *Green Chem.*, 2015, **17**, 1127–1135.

24 X. Xiao, B. W. Hoogendoorn, Y. Ma, S. A. Sahadevan, J. M. Gardner, K. Forsberg and R. T. Olsson, Ultrasound-assisted extraction of metals from lithium-ion batteries using natural organic acids, *Green Chem.*, 2021, **23**, 8519–8532.

25 T. Punt, S. M. Bradshaw, P. Van Wyk and G. Akdogan, Phase Separation in a novel selective lithium extraction from citrate media with D2EHPA, *Metals*, 2022, **12**, 1400.

26 W. Xuan, A. Chagnes, X. Xiao, R. T. Olsson and K. Forsberg, Antisolvent precipitation for metal recovery from citric acid solution in recycling of NMC cathode materials, *Metals*, 2022, **12**, 607.

27 S. Mallick, A. Patel, X.-G. Sun, M. P. Paranthaman, M. Mou, J. H. Mugumya, M. Jiang, M. L. Rasche, H. Lopez and R. B. Gupta, Low-cobalt active cathode materials for high-performance lithium-ion batteries: Synthesis and performance enhancement methods, *J. Mater. Chem. A*, 2023, **11**, 3789–3821.

28 H. Dong and G. M. Koenig, A review on synthesis and engineering of crystal precursors produced via coprecipitation for multicomponent lithium-ion battery cathode materials, *CrystEngComm*, 2020, **22**, 1514–1530.

29 V. Etacheri, in *Sol-Gel Materials for Energy, Environment and Electronic Applications*, ed. S. C. Pillai and S. Hehir, Springer, Cham, 2017, pp. 155–195.

30 M.-H. Lee, Y.-J. Kang, S.-T. Myung and Y.-K. Sun, Synthetic optimization of $Li[Ni_{1/3}Co_{1/3}Mn_{1/3}]O_2$ via co-precipitation, *Electrochim. Acta*, 2004, **50**, 939–948.

31 C. Deng, S. Zhang, B. L. Fu, S. Y. Yang and L. Ma, Synthetic optimization of nanostructured Li[Ni$_{1/3}$Mn$_{1/3}$Co$_{1/3}$]O$_2$ cathode material prepared by hydroxide coprecipitation at 273K, *J. Alloys Compd.*, 2010, **496**, 521–527.

32 L. Chang, W. Yang, K. Cai, X. Bi, A. Wei, R. Yang and J. Liu, A review on nickel-rich nickel–cobalt–manganese ternary cathode materials LiNi$_{0.6}$Co$_{0.2}$Mn$_{0.2}$O$_2$ for lithium-ion batteries: performance enhancement by modification, *Mater. Horiz.*, 2023, **10**, 4776–4826.

33 T. Wang, K. Ren, M. He, W. Dong, W. Xiao, H. Pan, J. Yang, Y. Yang, P. Liu, Z. Cao, X. Ma and H. Wang, Synthesis and manipulation of single-crystalline lithium nickel manganese cobalt oxide cathodes: A review of growth mechanism, *Front. Chem.*, 2020, **8**, 747.

34 L. Liang, K. Du, W. Lu, Z. Peng, Y. Cao and G. Hu, Synthesis and characterization of LiNi$_{0.6}$Co$_x$Mn$_{0.4-x}$O$_2$ (x = 0.05, 0.1, 0.15, 0.2, 0.25 and 0.3) with high-electrochemical performance for lithium-ion batteries, *Electrochim. Acta*, 2014, **146**, 207–217.

35 A. Purwanto, C. S. Yudha, U. Ubaidillah, H. Widiyandari, T. Ogi and H. Haerudin, NCA cathode material: Synthesis methods and performance enhancement efforts, *Mater. Res. Express*, 2018, **5**, 122001.

36 Q. Liu, H. Zhu, J. Liu, X. Liao, Z. Tang, C. Zhou, M. Yuan, J. Duan, L. Li and Z. Chen, High-performance lithium-rich layered oxide material: Effects of preparation methods on microstructure and electrochemical properties, *Materials*, 2020, **13**, 334.

37 B. Çetin, Z. Camtakan and N. Yuca, Synthesis and characterization of li-rich cathode material for lithium ion batteries, *Mater. Lett.*, 2020, **273**, 127927.

38 A. E. Abdel-Ghany, A. M. Hashem, A. Mauger and C. M. Julien, Effects of chelators on the structure and electrochemical properties of Li-rich Li$_{1.2}$Ni$_{0.13}$Co$_{0.13}$Mn$_{0.54}$O$_2$ cathode materials, *J. Solid State Electrochem.*, 2020, **24**, 3157–3172.

39 S. Dai, X. Li, J. Zhang and Z. Shao, Synthesis and electrochemical study of LiNi$_{1/3}$Co$_{1/3}$Mn$_{1/3}$O$_2$ cathode materials for lithium-ion batteries by polymer network gel method, *Colloids Surf.*, 2022, **643**, 128751.

40 D. He, Q. Guo, H. Yin, J. Li and Z. Gong, Sol-Gel Combustion Synthesis of Li$_{1.2}$Mn$_{0.54}$Ni$_{0.13}$Co$_{0.13}$O$_2$ as Cathode Materials for Lithium Ion Batteries, *Int. J. Electrochem. Sci.*, 2017, **12**, 455–465.

41 D. Jiang, L. Zhao, Y. Shao and D. Wang, Preparation and characterization of layered LiNi$_{0.9}$Co$_{0.05}$Mn$_{0.025}$Mg$_{0.025}$O$_2$ cathode material by a sol–gel method for lithium-ion batteries, *RSC Adv.*, 2015, **5**, 40779–40784.

42 J. Yu, J. Li, S. Zhang, F. Wei, Y. Liu and J. Li, Mechanochemical upcycling of spent LiCoO$_2$ to new LiNi$_{0.80}$Co$_{0.15}$Al$_{0.05}$O$_2$ battery: An atom economy strategy, *Proc. Natl. Acad. Sci. U. S. A.*, 2023, **120**, e2217698120.

43 Y.-J. Shih, S.-K. Chien, S.-R. Jhang and Y.-C. Lin, Chemical leaching, precipitation and solvent extraction for sequential separation of valuable metals in cathode material of spent lithium ion batteries, *J. Taiwan Inst. Chem. Eng.*, 2019, **100**, 151–159.

44 H. Tyagi, A. Kushwaha, A. Kumar and M. Aslam, A facile pH controlled citrate-based reduction method for gold nanoparticle synthesis at room temperature, *Nanoscale Res. Lett.*, 2016, **11**, 362.

45 C. Ma, J. D. Gamarra, R. Younesi, K. Forsberg and M. Svärd, Antisolvent crystallization from deep eutectic solvent leachates of LiNi$_{1/3}$Co$_{1/3}$Mn$_{1/3}$O$_2$ for recycling and direct synthesis of battery cathodes, *Resour., Conserv. Recycl.*, 2023, **198**, 107210.

46 R. I. Bickley, H. G. M. Edwards, R. Gustar and S. J. Rose, A vibrational spectroscopic study of nickel (II) citrate Ni$_3$(C$_6$H$_5$O$_7$)$_2$ and its aqueous solutions, *J. Mol. Struct.*, 1991, **246**, 217–228.

47 Z. Kartal, O. Şahin and A. Yavuz, Synthesis, crystal structure, and characterization of two heterometallic transitionmetal citrate complexes [M=Co(II) and Cd(II)], *Turk. J. Chem.*, 2019, **43**, 555–567.

48 E. Delahaye, R. Moulin, M. Aouadi, V. Trannoy, P. Beaunier, G. Fornasieri and A. Bleuzen, Co2+@mesoporous silica monoliths: Tailor-made nanoreactors for confined soft chemistry, *Chem.–Eur. J.*, 2015, **21**, 16906–16916.

49 X. Zhang, W. J. Jiang, A. Mauger, Qilu, F. Gendron and C. M. Julien, Minimization of the cation mixing in Li$_{1+x}$(NMC)$_{1-x}$O$_2$ as cathode material, *J. Power Sources*, 2010, **195**, 1292–1301.